Supporting Information

Exposure of V Sites on $InVO_4$ via Rapid Joule-Heating for Highly Efficient Photocatalytic N_2 Fixation

Qianyu Chu[1], Guangmin Ren[3], Jingdan Zhao[1], Xiangchao Meng[1], Jie Meng[2*] and Zizhen Li[1*]

[1]Key Laboratory of Marine Chemistry Theory and Technology (Ministry of Education), College of Chemistry & Chemical Engineering, Ocean University of China, Qingdao, Shandong, 266100, China.

[2]School of Mathematical Sciences, Ocean University of China, Qingdao 266100, China

[3]State Key Laboratory Base of Eco-Chemical Engineering, College of Chemical Engineering, Qingdao University of Science & Technology, Qingdao, 266042, China

**Corresponding author*

E-mail: mengjie@ouc.edu.cn (J.M.); lizizhen@ouc.edu.cn (Z.L.)

Experimental Section

Characterizations

The X-ray diffraction (XRD) patterns were collected on a Rigaku Miniflex 600. The morphology of the prepared samples was shown on a Hitachi S-4800 field emission scanning electron microscope (SEM). Transmission electron microscopy (TEM) was obtained using a scanning electron microscope (FE-SEM SU-8010) and a transmission electron microscope (TEM, Talos-F200X). Electron paramagnetic resonance (EPR) spectra were obtained on a Bruker-A300/E500. X-ray photoelectron spectroscopy (XPS) data were obtained using a Thermo Fisher Scientific-ESCALAB 250Xi. In situ X-ray photoelectron spectroscopy (In situ XPS) data were obtained using a Thermo Scientific ESCALAB 250Xi. The UV-Vis diffuse reflectance spectra (DRS) were obtained by measurement using a PUXI TU-1901 spectrometer with $BaSO_4$ as a reference. Thermogravimetry (Netzsch STA449F3) was used to study the weight loss of a sample as a function of temperature. The in situ DRFT-IR spectra were recorded using an in situ FTIR spectrometer (Thermo iS50FT-IR) equipped with an MCT detector and a specially designed reaction cell.

Electrochemical measurements

Photoelectrochemistry experiments use a 300 W xenon lamp as the light source. Transient photocurrent response measurements and electrochemical impedance spectroscopy (EIS) of samples were measured using the CHI 660E electrochemical workstation. Measurements were performed using a three-electrode system (reference electrode (saturated calomel electrode), counter electrode (graphite electrode), and working electrode) in 0.5 mol/L Na_2SO_4 solution. The working electrode was prepared as follows: 10 mg of catalyst was dispersed in a mixture of 200 ml of deionized water and 20 μl of Nafion, and then the suspension was applied on a clean FTO conductive glass (1 × 1 cm) to dry naturally.

The DFT calculation details

In order to reveal the mechanism of NRR on the surface of $InVO_4$-JH, the first principle calculations were performed, by using the projector augmented wave pseudopotentials and Perdew-Burke-Ernzerhof exchange-correlation as implemented in the Vienna ab initio simulation package (VASP)[1, 2]. The generalized gradient approximation method of Perdew-Burke-Ernzerhof (PBE) functional was used to describe the exchange-related interaction between electrons[3]. A 3 × 3 × 1 $InVO_4$ super- cell is adopted for slab modeling and the (1 1 2) plane was denoted as $InVO_4$ (1 1 2). Then, a vacuum of 15Å width was added in the direction normal to the surfaces. The O atom is removed based on $InVO_4$ (1 1 2) to further simulate the oxygen-vacancy $InVO_4$-JH. The convergence criteria for the total energy and the Hellmann-Feynman force were 10-5 eV and 0.02 eV, respectively. For energy calculations, the Brillouin zone was sampled with a 3 × 3 × 1 Gamma-center k-point mesh. The Gibbs free-energy change for the relevant elemental steps was calculated by a computational hydrogen electrode model, which can also be obtained by $\Delta G = \Delta E + \Delta E_{ZPE} - T\Delta S$, where ΔE is the total energy, ΔE_{ZPE} is the zero-point energy and S is the entropy at 298.15 K. Zero-point energy corrections and entropic contributions to the free energies (T=298.15 K).

Figures

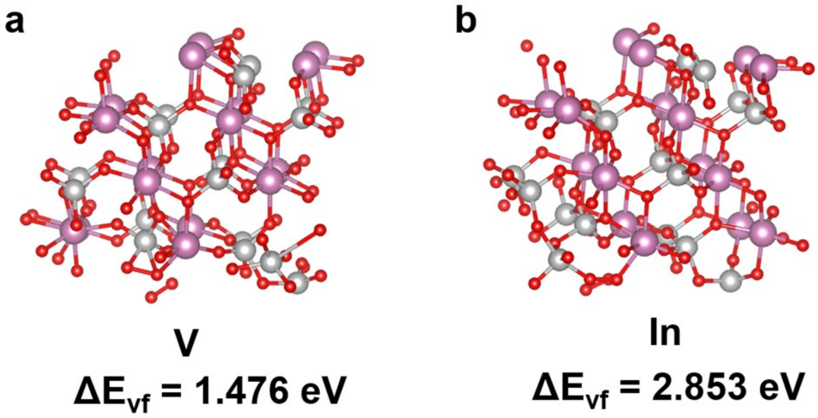

Figure S1. Oxygen vacancy formation energies in indium vanadate for (a) V, (b) In.

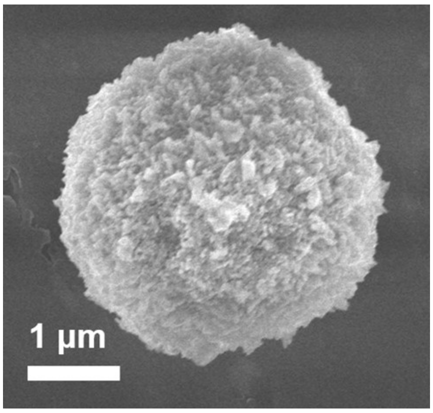

Figure S2. SEM image of primary $InVO_4$.

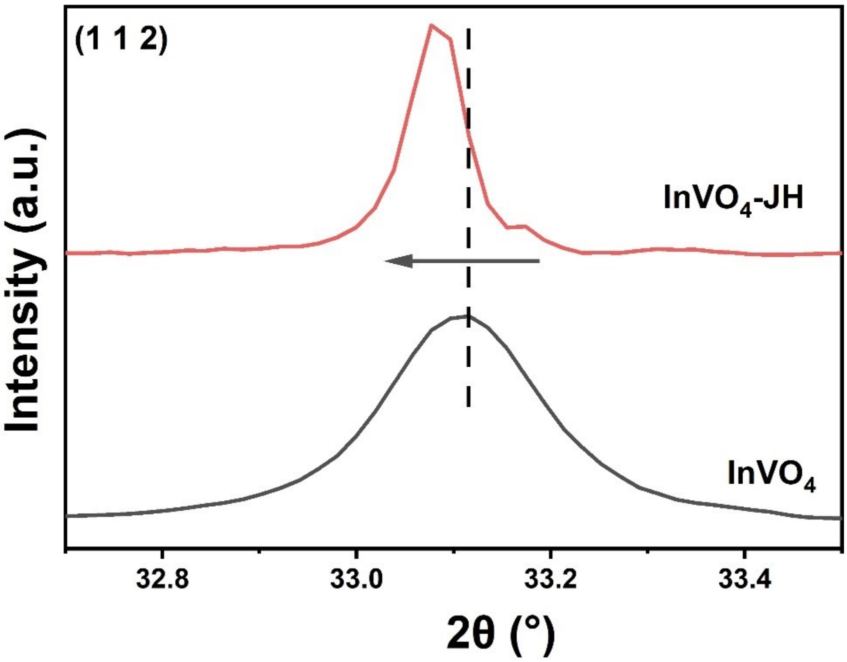

Figure S3. XRD partial enlargement of the (1 1 2) main peak for $InVO_4$ and $InVO_4$-JH.

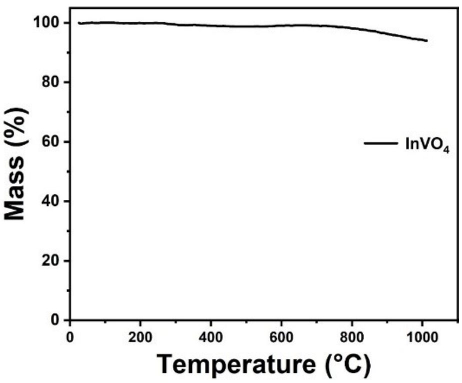

Figure S4. TGA curves of $InVO_4$.

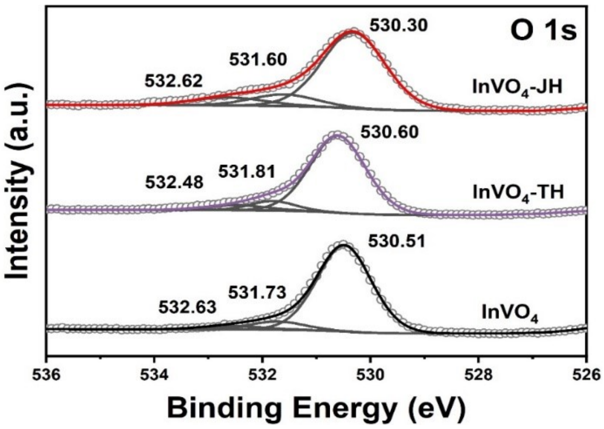

Figure S5. XPS spectra of O 1s in $InVO_4$, $InVO_4$-TH and $InVO_4$-JH.

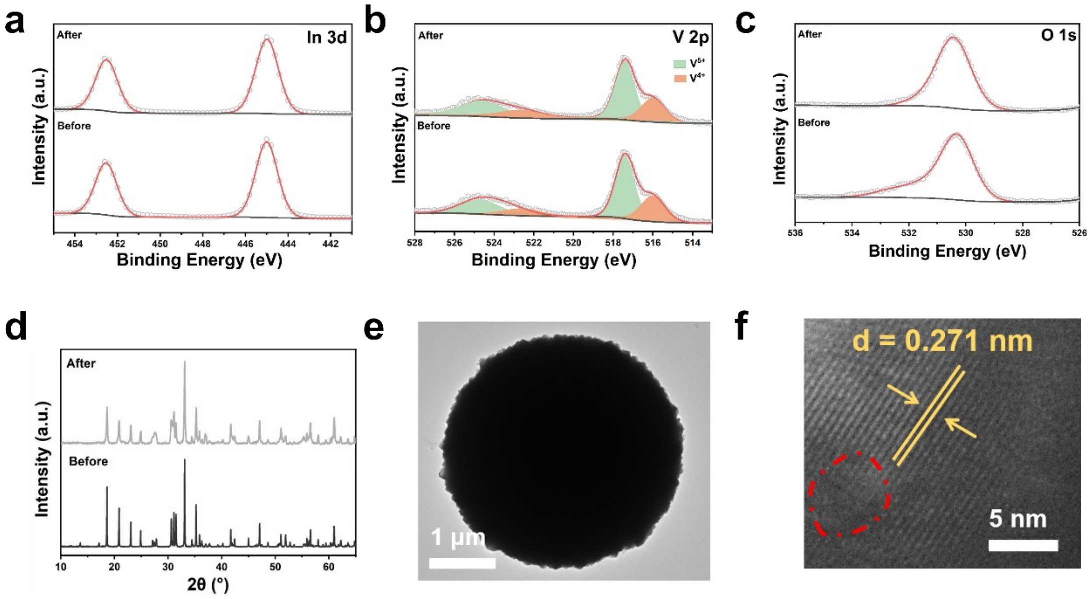

Figure S6. Reacted $InVO_4$-JH XPS spectra of (a) In 3d, (b) V 2p, (c) O 1s, (d)XRD, (e-f) TEM.

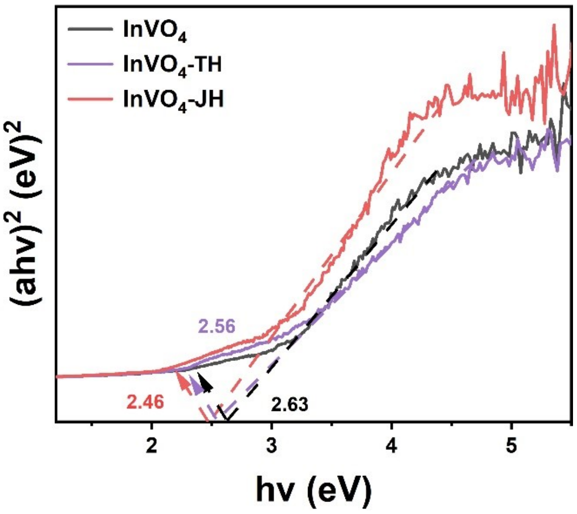

Figure S7. Tauc plots of $(\alpha h\nu)^2$ versus energy (hν) of $InVO_4$, $InVO_4$-TH and $InVO_4$-JH.

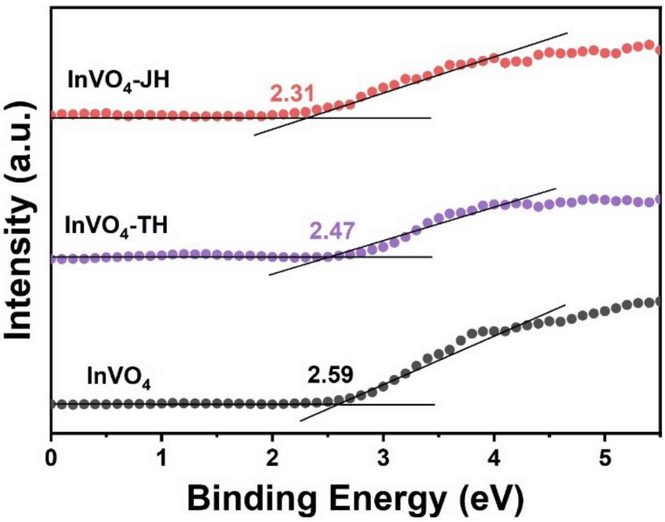

Figure S8. XPS valence spectra of InVO$_4$, InVO$_4$-TH and InVO$_4$-JH.

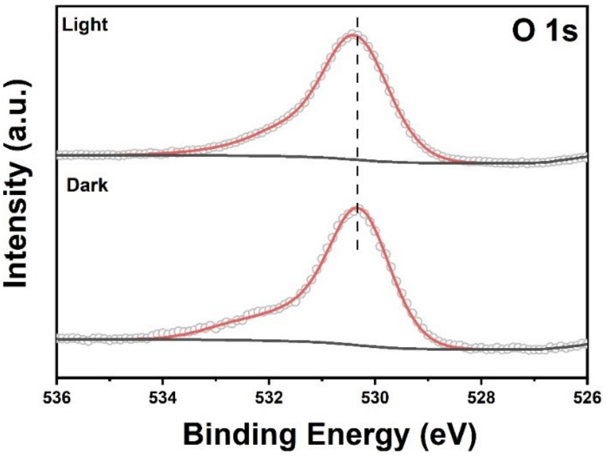

Figure S9. In-situ XPS spectra of InVO4-JH for O 1s.

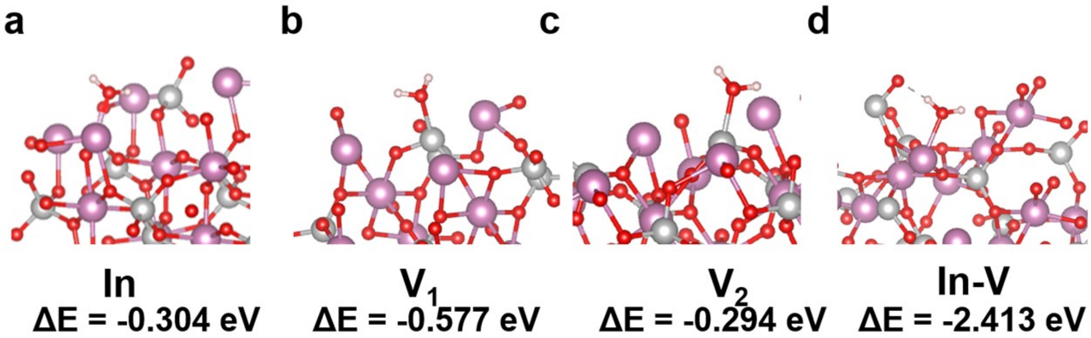

Figure S10. Adsorption energy of water molecules at different sites in $InVO_4$.

Table S1. Compositional analysis from V 2p spectra.

Photocatalyst	Constituents Present in %		Ratio
	V^{5+}	V^{4+}	V^{4+}/V^{5+}
$InVO_4$	90.05	9.95	0.11
$InVO_4$-TH	71.90	28.10	0.39
$InVO_4$-JH	67.01	32.99	0.49

References:

[1] Kresse, G.; Furthmüller, J. Efficiency of Ab-Initio Total Energy Calculations for Metals and Semiconductors Using A Plane-Wave Basis Set. Comp. Mater. Sci. 1996, 6, 15-50. [J].

[2] Kresse, G.; Furthmüller, J. Efficient Iterative Schemes for Ab Initio Total-Energy Calculations Using A Plane-Wave Basis Set. Phys. Rev. B 1996, 54, 11169. [J].

[3] Perdew, J. P.; Burke, K.; Ernzerhof, M. Phys. Generalized Gradient Approximation Made Simple. Rev. Lett. 1996, 77, 3865-3868. [J].